Energy and Buildings xxx (2013) xxx–xxx

Contents lists available at ScienceDirect

Energy and Buildings

journal homepage: www.elsevier.com/locate/enbuild

Graphical Abstract

Energy and Buildings xxx (2013) xxx–xxx

Hygrothermal study of lightweight concrete hollow bricks: A new proposed experimental–numerical method

J.J. del Coz Díaz*, F.P. Álvarez Rabanal, O. Gencel, P.J. García Nieto, M. Alonso Martínez, A. Navarro Manso, B. Prendes-Gero

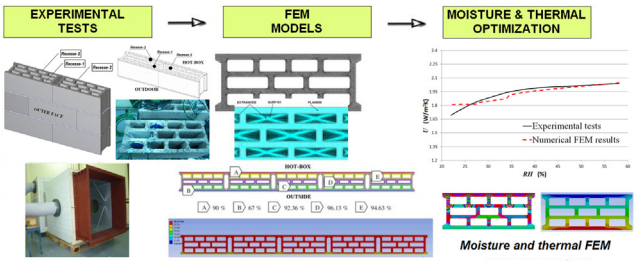

Energy and Buildings xxx (2013) xxx–xxx

Contents lists available at ScienceDirect

Energy and Buildings

journal homepage: www.elsevier.com/locate/enbuild

Highlights

Energy and Buildings xxx (2013) xxx–xxx

Hygrothermal study of lightweight concrete hollow bricks: A new proposed experimental–numerical method

J.J. del Coz Díaz*, F.P. Álvarez Rabanal, O. Gencel, P.J. García Nieto, M. Alonso Martínez, A. Navarro Manso, B. Prendes-Gero

- A new hygrothermal test procedure based on hot-box apparatus is presented.
- The hygrothermal behavior of a multi-holed wall is solved by FEM–DOE–GDO methodology.
- This new hybrid method saves a 70% of energy and time with respect to current tests.
- The numerical and experimental results have shown a very good agreement.

Energy and Buildings xxx (2013) xxx–xxx

Contents lists available at ScienceDirect

Energy and Buildings

journal homepage: www.elsevier.com/locate/enbuild

Hygrothermal study of lightweight concrete hollow bricks: A new proposed experimental–numerical method

Q1 J.J. del Coz Díaz[a,*], F.P. Álvarez Rabanal[a], O. Gencel[b], P.J. García Nieto[c], M. Alonso Martínez[a], A. Navarro Manso[d], B. Prendes-Gero[a]

[a] Department of Construction, EPSIG, University of Oviedo, Departmental Building 7, 33204 Gijón, Spain
[b] Civil Engineering Department, Faculty of Engineering, Bartin University, 74100 Bartin, Turkey
[c] Department of Mathematics, Faculty of Sciences, University of Oviedo, 33007 Oviedo, Spain
[d] Department of Energy, University of Oviedo, 33204 Gijón, Spain

ARTICLE INFO

Article history:
Received 6 May 2013
Received in revised form 13 October 2013
Accepted 18 November 2013

Keywords:
Finite element modeling
Light concrete hollow bricks
Nonlinear numerical simulation
Coupled hygrothermal analysis
Hygrothermal tests
Porous media

ABSTRACT

The aim of this paper is the development of a new hybrid methodology to study the moisture transport and heat transfer in masonry structures made up of light concrete hollow bricks (LWHBs) from the numerical and experimental points of view. In order to solve this coupled nonlinear hygrothermal analysis, an instrumented one square meter wall was subjected to eight different moisture stages in the laboratory using a special testing device during a total time of 1480 h. In order to simulate the different experimental stages, steady and transient states were implemented in the finite element models. Furthermore, the design of experiments methodology (DOE) and the goal design optimization (GDO) technique are used to calculate the best optimal parameters from the laboratory tests. Once the optimal parameters have been obtained, the finite element models for each stage are solved so that the moisture and temperature distributions were calculated. In this sense, a very good agreement between the numerical and experimental results is achieved. Finally, the most important conclusions of this study and advantages of this new methodology are exposed.

1. Introduction

The present research work tackles the study of the hygrothermal efficiency of the porous lightweight concrete material (LWHC) [1] and the effect of the moisture transport on the thermal performance of walls made up of lightweight concrete hollow blocks (LWHB) [2,3]. In the framework considered here, light concrete material is more and more recommended by the builders to reach a sustainable development due to their good strength and thermal properties [4,5]. Department of Public Works as well as owners and building proprietors are demanding high-capacity heat-insulating exterior masonry components specifically for further energy savings. For housing as well as in civil and industrial structures, there is also a great interest in light building materials with good physical material behavior, with respect to an energy conscious and ecological design, which fulfills all strength and serviceability requirements, including its thermal and moisture performance.

In recent years, many research works have been published about the exposure of buildings to the driving rain and water penetration [6–8]. These environmental phenomena give place to the decreasing in the facade durability and the hygrothermal behavior [9,10], and therefore reducing the insulation performance and energy savings. With respect to the LWHB's hygrothermal properties, when the density and thermal conductivity are decreased, the porous structure and the hygroscopic sorption are increased. This phenomenon gives rise to an important reduction in the thermal performance of the LWHBs, according to the previous research works [2,11].

Therefore, it is necessary to build a model that allows an accurate and entire description of the coupled problem in relation to the storage and transport of heat and moisture inside lightweight concrete wall. This phenomenon is strongly linked to both temperature and humidity of the surrounding environment as well as its current structure of pores. In this sense, the variations of the external conditions change the temperature in the lightweight concrete mass and the moisture movement within this material. These variations take place until equilibrium is reached between the structure and environment. Both the hygrothermal state of the lightweight concrete and its porous structure causes different mechanisms of moisture transport and storage. The exact description of these phenomena becomes difficult because the most influential factors have both the geometrical and temporal dependence. Taking into account the

* Corresponding author. Tel.: +34 985 182042; fax: +34 985 182433.
E-mail addresses: delcoz@uniovi.es, juanjo@constru.uniovi.es (J.J. del Coz Díaz).

0378-7788/$ – see front matter © 2013 Published by Elsevier B.V.
http://dx.doi.org/10.1016/j.enbuild.2013.11.060

Nomenclature

A	surface of a specific recess or cavity (m^2)
D_m	moisture diffusion coefficient or material diffusivity (m^2/s)
$D_{m_{vap}}$	isothermal vapor diffusivity (m^2/s)
D_θ	thermal moisture diffusion coefficient (kg/(m s K))
e	specimen thickness in the heat transfer direction (m)
F_m	conversion factor for the moisture content (dimensionless)
h_v	latent heat of vaporization (J/kg)
h_{coz}	equivalent moisture film coefficient (s^{-1})
h_{coz}^{Ri}	equivalent moisture film coefficient in the recess "i" (s^{-1})
LWA	lightweight aggregate
LWHB	lightweight hollow brick
m	moisture content (kg/m^3)
Q	heat flux, or heat flow rate through a surface of unit area perpendicular to the direction of heat flow (W/m^2)
q_{conv}	thermal convective flow (W/m^2)
q_{coz}	convective equivalent empirical moisture flow (kg/m s)
q_{rad}	thermal radiation flow (W/m^2)
R	overall thermal resistance (m^2 K/W)
R_{se}	surface thermal resistance of the specimen on the inner face (hot-box) (m^2 K/W)
R_{si}	surface thermal resistance of the specimen on the outer face (lab room conditions) (m^2 K/W)
RH	relative humidity or moisture potential (%)
RMSE	root mean squared error
ΔT	temperature difference between the inner (hot-box) and the outer faces (K)
t	time (s)
U	heat transmission coefficient or thermal transmittance (W/m^2 K)

Greek symbols

λ	thermal conductivity (W/m K)
$\lambda_{50\%}$	thermal conductivity for RH = 50% (W/m K)
λ_{eq}	equivalent thermal conductivity of the brick (W/m K)
ρ	material density (kg/m^3)
ρc	volumetric heat capacity ($J/(m^3$ K))
θ	temperature (K)
θ_i	wall temperature inside a cavity (K)
θ_j	air temperature inside a cavity (K)

transportation laws, it is possible to derive the differential equations of equilibrium able to describe rightly the key mechanisms of the transport and storage.

In order to solve this problem, a hybrid methodology using numerical and experimental methods in combination has been developed [12–15]. On the one hand, it is necessary to obtain the experimental hygrothermal properties of an instrumented entire wall made up of LWHBs under different moisture contents. On the other hand, the numerical problem implies the solution of two simultaneous nonlinearities [1,3]: the material nonlinearity (i.e., most building materials have variable hygrothermal material properties) and radiation and convection boundary conditions inside recesses (inner holes) of the bricks [14,16,17]. The governing equations that describe the moisture diffusion coupled with the heat conduction in porous solids are well-known [18–20]. To solve this highly nonlinear coupled problem, a goal driven optimization (GDO) approach based on the finite element method (FEM) in combination with the design of experiments (DOE) analysis has been used with success [21–23].

This research work is structured as follows: firstly, the materials and experimental methods used to carry out this study are described; secondly, the mathematical and numerical models are written; thirdly, the numerical results and the DOE optimization are presented and discussed; and finally, the main conclusions drawn from the experimental and numerical results are exposed.

Table 1
Physical properties and mix proportions of the lightweight hollow bricks (LWHBs).

	Corner brick	Normal brick
Height (m)	0.195	0.195
Length (m)	0.5	0.5
Width (m)	0.195	0.195
Mean weight (kg)	13.63	12.80
Real mean density (kg/m^3)	1329	1329
LWA (kg)	3.25	3.06
Silica sand (kg)	8.28	7.80
Cement (kg)	2.00	1.90
Water (kg)	1.50	1.40

Note: LWA (lightweight aggregate): 4–12.5 mm particle diameter (expanded clay).

2. Materials and experimental methods

2.1. Hollow bricks and laboratory tests

The materials used in this research work include lightweight hollow bricks (LWHB) (see Fig. 1(a)) manufactured with expanded clay (main lightweight aggregate), cement and silica sand. The particle size of the expanded clay ranges from 4 to 12.5 mm for lightweight aggregate and from 1 to 5 mm for lightweight sand, respectively. The main properties as well as the overall dimensions of the two types of LWHBs are shown in Table 1 and Fig. 1(a).

With the above indicated LWHBs, a one square meter wall is built and placed over a steel frame in order to check its hygrothermal performance (see Fig. 1(b)). A total of 11 hygrothermal microsensors (see Fig. 1(c)) as well as 7 heat flux sensors with thermocouples (see Fig. 1(d)) are located in this wall at specific places (inner face, outer face and inside wall recesses) (see Fig. 1(e) and (f)) in order to obtain the temperature, relative humidity and thermal fluxes at different locations in the laboratory tests [24,25]. Our laboratory facilities include a climatic air-conditioned system so that the temperature remains constant (about 18 ± 2 °C) during the hygrothermal tests.

With respect to the hygrothermal test, the main stages are as follows (see the flowchart in Fig. 2):

1. *Humidity wall stabilization*: once the wall is built, the wall is placed in our laboratory at its thermal and moisture conditions for 10 days.
2. *Wall drying*: The wall is located in the hot-box apparatus and connected to a special climatic chamber device. A relative humidity of 10% and a 60 °C temperature are kept constant during additional ten days inside the climatic chamber in order to dry the wall. The overall time of the first and second stages (humidity wall stabilization and wall drying) is enough to reach the steady-state conditions (20 days in total). As it is possible to observe in Fig. 3(a), the relative humidity in the inner face (hot-box) remains constant (about 10% of RH).
3. *Thermal conductivity test*: Six stages at different moisture contents (10%, 30%, 50%, 65%, 80% and 90%, respectively) are checked at a constant temperature of 55 °C inside the hot-box. Each stage

Please cite this article in press as: J.J. del Coz Díaz, et al., Hygrothermal study of lightweight concrete hollow bricks: A new proposed experimental–numerical method, Energy Buildings (2013), http://dx.doi.org/10.1016/j.enbuild.2013.11.060

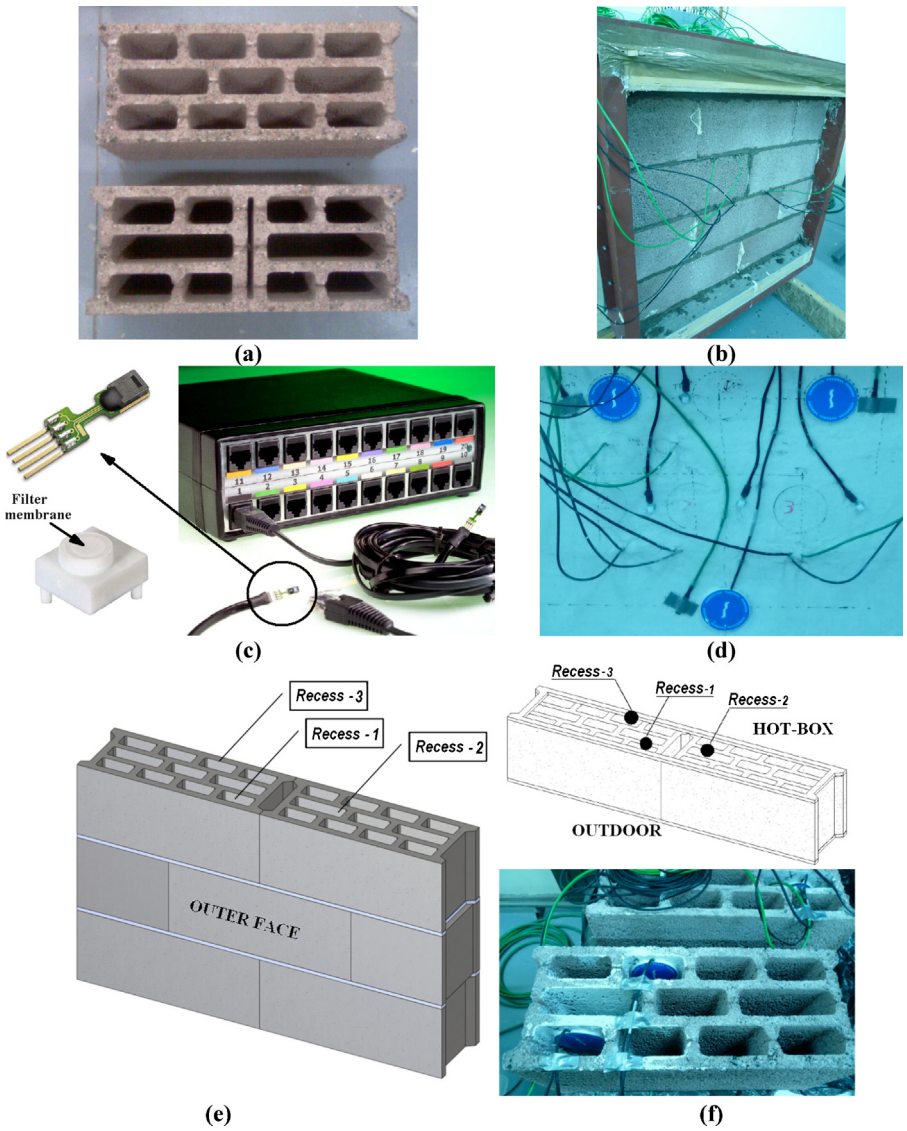

Fig. 1. Laboratory setup: (a) picture of the normal brick (upper) and corner brick (lower); (b) wall tested; (c) hygrothermal microsensors and datalogger; (d) heat flux sensors with thermocouples; (e) name of recesses; and (f) a detail of interior heat flux sensors.

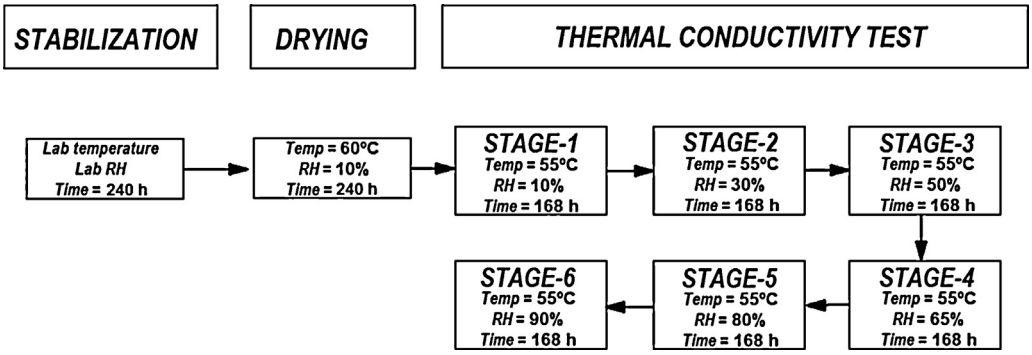

Fig. 2. Flowchart of the laboratory tests.

takes over 7 days and the thermal conductivity test takes over 42 days.

The total time in each stage is calculated based on the speed of response of the testing apparatus and specimen's response to changes in its environmental conditions. In this sense, taking into account the standard rule requirements [25] and current researches in this field [26,27], it is possible to conclude that 72 h are enough to achieve the stabilization in thermal conductivity tests. Indeed, the results obtained in our tests confirm this specific point.

Please cite this article in press as: J.J. del Coz Díaz, et al., Hygrothermal study of lightweight concrete hollow bricks: A new proposed experimental–numerical method, Energy Buildings (2013), http://dx.doi.org/10.1016/j.enbuild.2013.11.060

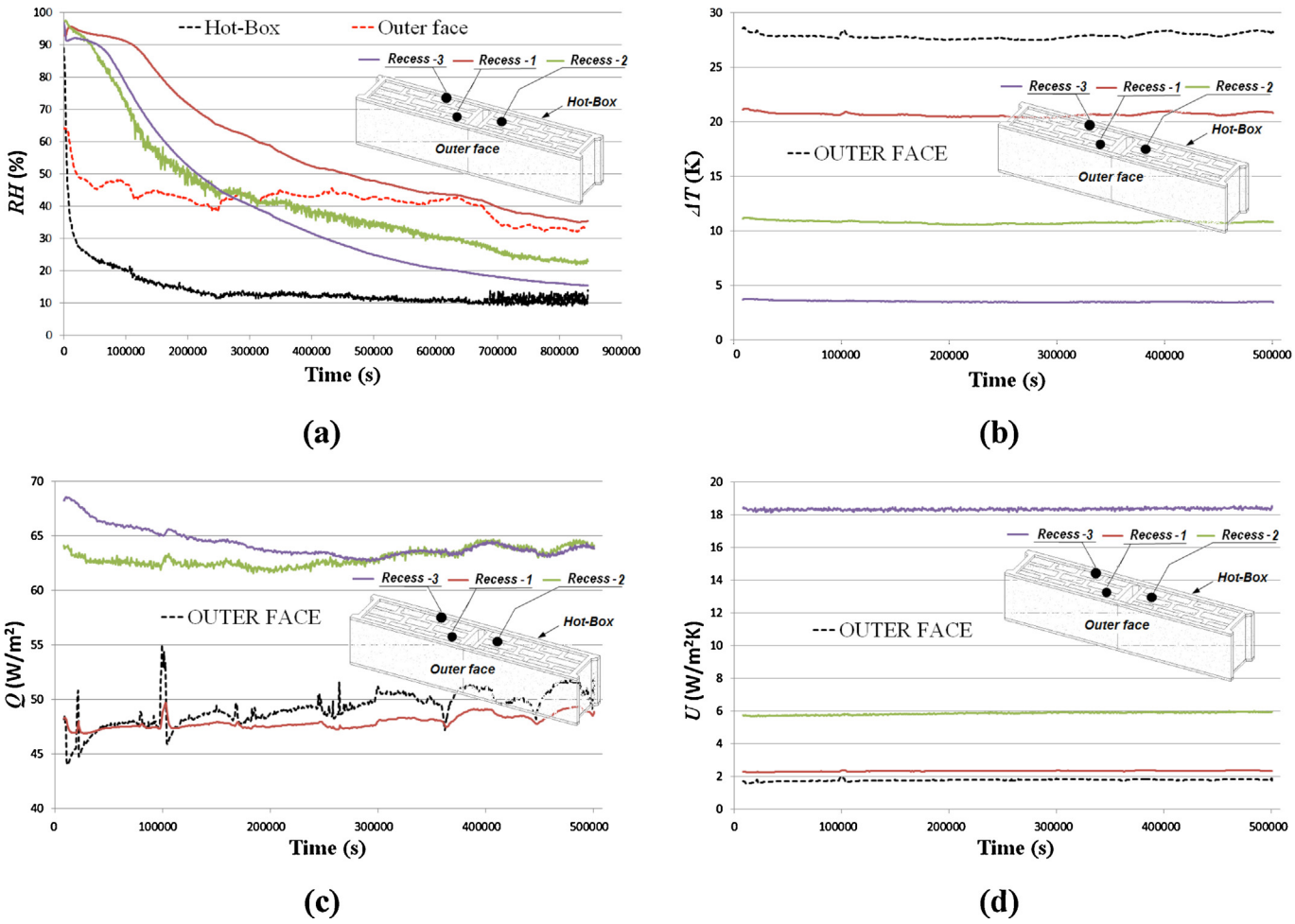

Fig. 3. Experimental results during the wall drying stage versus time curves: (a) relative humidity; (b) temperature differences; (c) thermal flux and (d) thermal transmittance.

2.2. Experimental results

On the one hand, Fig. 3 shows the curves obtained from the laboratory tests for the two first stages (humidity wall stabilization and wall drying). These curves correspond to the relative humidity (RH) (Fig. 3(a)), temperature differences (ΔT) (Fig. 3(b)), thermal flux (Fig. 3(c)) and thermal transmittance (Fig. 3(d)) as a function of time for the three different recesses as well as the outer and inner (hot-box) wall faces, respectively.

Firstly, it is possible to observe in Fig. 3(a) that the wall relative humidity decreases over the time during the drying process, reaching the minimum 10% RH value inside hot-box apparatus at the end of the test. Secondly, Fig. 3(b) indicates the test's temperature differences. Thirdly, the thermal fluxes shown in Fig. 3(c) have been stable in this stage. Finally, Fig. 3(d) shows the thermal transmittances of the wall over the time. Note that it is mandatory to fulfill the constraint $\Delta T \geq 15$ K [24,25] to calculate the heat transmission coefficient. Therefore, only the data provided by the sensors located in the recess 1 and outer face must be taken into account for the U calculations.

On the other hand, the curves corresponding to each content of moisture in the hot-box are shown in Fig. 4. These curves indicate the relative humidity (Fig. 4(a)), temperature differences between the inner face and the remaining faces (Fig. 4(b)), thermal flux (Fig. 4(c)) and thermal transmittance (Fig. 4(d)) versus time for the six different stages of the thermal conductivity tests, respectively.

In the first place, Fig. 4(a) indicates the relative humidity evolution during the six different stages, ranging from 10% to 95% RH values inside hot-box apparatus. In the second place, Fig. 4(b) shows that the temperature differences are almost constant during the experimental test. Thirdly, Fig. 4(c) shows the thermal flux curves with small fluctuations due to the climatic chamber's operation, although the general trend is monotonically decreasing. Finally, Fig. 4(d) shows the thermal transmittances of the wall during the six thermal conductivity test stages. Similar to the previous Fig. 3(d), the same constraint $\Delta T \geq 15$ K has to be considered, so that only recess 1 and outer face U values are taking into account.

3. Mathematical and numerical models

Keeping in mind some studies of finite element analysis applied to the solution of the hygrothermal nonlinear problem, it is instructive to recall the first mathematical formulation of the equations that governing the phenomena analyzed [18,19].

3.1. Governing equilibrium equations

For many years, the phenomenon of moisture and heat transfer in porous media has been studied in the science and engineering research community. A comprehensive approach in modeling the moisture and heat transports was developed by Philip and De Vries [18,19] which considers the moisture movement in both vapor and liquid phases using Fick's and Darcy's laws, respectively. The proposed governing equation was separated into two components defining the mechanisms for isothermal moisture diffusion and heat-induced moisture diffusion. This approach gives place to

Please cite this article in press as: J.J. del Coz Díaz, et al., Hygrothermal study of lightweight concrete hollow bricks: A new proposed experimental–numerical method, Energy Buildings (2013), http://dx.doi.org/10.1016/j.enbuild.2013.11.060

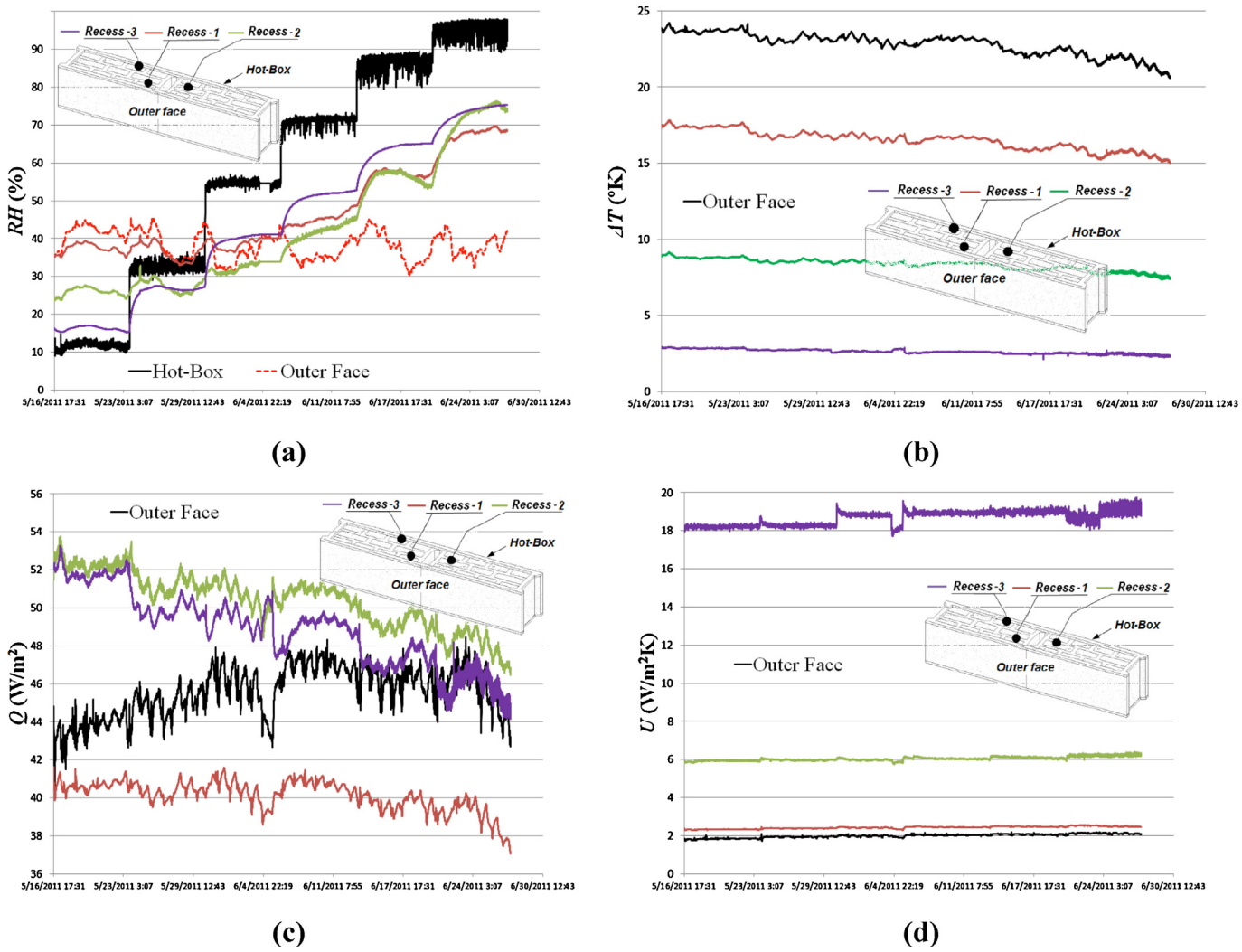

Fig. 4. Experimental results for the six different thermal conductivity stages to each content of moisture in the hot-box versus time: (a) relative humidity; (b) temperature difference; (c) thermal flux and (d) thermal transmittance.

a system of coupled partial differential equations consisting of a moisture transfer equation and a heat balance equation as follows [20,26]:

$$\frac{\partial m}{\partial t} = \nabla \cdot (D_m \nabla m) + \nabla \cdot (D_\theta \nabla \theta) \quad (1)$$

$$\rho c \frac{\partial \theta}{\partial t} = \nabla \cdot (\lambda \nabla \theta) + h_v \nabla \cdot (D_{m_{vap}} \nabla m) \quad (2)$$

Despite the lack of rigorous definition for the measurement for the coefficient of thermal moisture definition, D_θ, the Philip and De Vries model [19] has gained wide spread popularity in the literature. In the moisture transport equation, Eq. (1), the first term on the right hand side of the equation represents the moisture movement due to moisture gradient, while the second term describes the moisture movement due to temperature gradient.

In order to solve the partial differential equation coupled system given by Eqs. (1) and (2), we have applied here the physical analogy between the moisture and thermal transport based on the Fick's law [18,20].

On the one hand, it is necessary taking into account the following main hypotheses:

H1. Moisture transport takes place through a non-homogeneous porous non-saturated medium (solid plus air).

H2. The thermal gradient is small enough so that the moisture transport due to the thermal moisture diffusion coefficient is negligible.

H3. It is assumed that in all cases of this research work is being far away from the dew point.

H4. A linear relationship between moisture content and relative humidity is assumed in the interval considered (from 10% to 90% RH values) as it was experimentally proved in previous works [11,20].

H5. It has been postulated in the literature that the sorption isotherm describing the variation of moisture content in a porous medium with respect to relative humidity of the surrounding air has a negligible dependency to temperature. Based on this consideration, the relative humidity, RH, of the surrounding air was used as the moisture potential of the current research work [27].

Applying the change of variables from moisture content to relative humidity moisture potential, RH:

$$\nabla m = \frac{\partial m}{\partial \mathrm{RH}} \nabla \mathrm{RH} \quad \text{and} \quad \frac{\partial m}{\partial t} = \frac{\partial m}{\partial \mathrm{RH}} \cdot \frac{\partial \mathrm{RH}}{\partial t} \quad (3)$$

Eq. (1), corresponding to the moisture transport, is reduced to the following nonlinear equation taking into account Eq. (3) and

Please cite this article in press as: J.J. del Coz Díaz, et al., Hygrothermal study of lightweight concrete hollow bricks: A new proposed experimental–numerical method, Energy Buildings (2013), http://dx.doi.org/10.1016/j.enbuild.2013.11.060

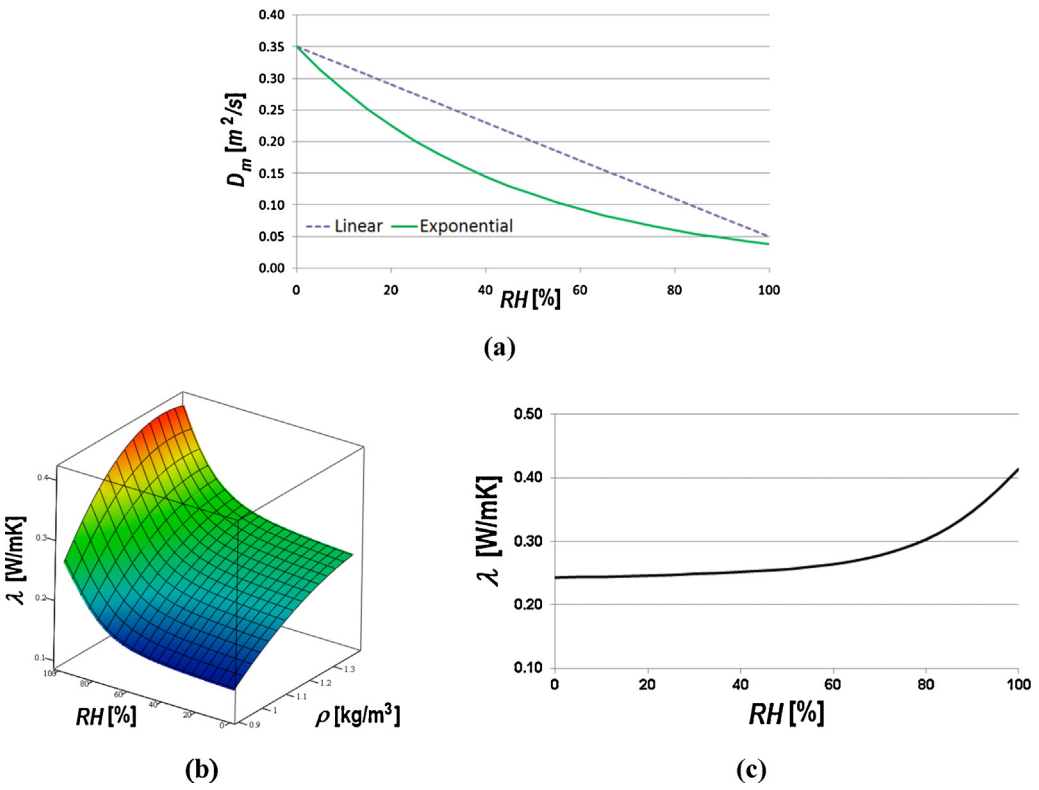

Fig. 5. Material properties of the LWHB: (a) material diffusivity laws as a function of the moisture content (%); (b) thermal conductivity surface (W/m K) as a function of light concrete density (kg/m^3) and relative humidity (%); and (c) thermal conductivity curve as a function of the moisture content for a density of 1329 kg/m^3.

the hypotheses H1–H5:

$$\frac{\partial m}{\partial t} = \nabla \cdot (D_m \nabla m) + \nabla \cdot (D_\theta \nabla \theta) \overset{\text{H1–H5}}{\Rightarrow} C^*_{\text{RH}} \frac{\partial \text{RH}}{\partial t} = \nabla \cdot (D_{\text{RH}}(m) \nabla \text{RH}) \tag{4}$$

On the other hand, the following hypotheses are taking into account to solve the thermal transport in this work:

H6. Thermal conductivity is moisture-dependent [11].

H7. Furthermore, we neglect the effect of latent heat diffusion [20].

Eq. (2), corresponding to the heat balance transport, is transformed to the following equation taking into account the two previous hypotheses H6 and H7:

$$\rho c \frac{\partial \theta}{\partial t} = \nabla \cdot (\lambda \nabla \theta) + h_v \nabla \cdot (D_{m_{\text{vap}}} \nabla m) \overset{\text{H6–H7}}{\Rightarrow} \rho c \frac{\partial \theta}{\partial t} = \nabla \cdot (\lambda(m) \nabla \theta) \tag{5}$$

It might be noted here that the above governing equilibrium equations are solved using the finite element method (FEM).

3.2. Material: properties and models

In order to integrate the previous governing equations, Eqs. (3) and (4), it is necessary to take into account the relationship between the moisture diffusion coefficient or material diffusivity (D_m) and the material thermal conductivity (λ) as a function of the relative humidity (RH). Keeping in mind this fact, Fig. 5(a) shows two material diffusivity laws of the LWHB as a function of the moisture content (in percentage) [8]. Fig. 5(b) indicates the thermal conductivity as a function of the light concrete density (kg/m^3) and moisture content, and finally Fig. 5(c) shows the thermal conductivity as a function of the moisture content [11].

It is possible to observe that the moisture diffusion coefficient of light concrete decreases as the moisture content increases until the block is saturated. Furthermore, the thermal conductivity of light concrete increases as the equivalent density grows (see Fig. 2 right).

The main parameters to be used in the numerical simulation are (see Fig. 2):

- *Density, ρ (kg/m^3)*: Calculated from the mean weight of the LWHB used (see Table 1).
- *Moisture diffusivity, D_m (m^2/s)*: Based on the Fick's law for the moisture transport in porous media. It is possible to conclude that the moisture diffusivity through a wall is inversely proportional to the density. In this research work, we have used two different moisture-diffusivity approaches (see Fig. 5(a)):
  - *Linear equation*: Based on the following expression $D_m = a + b \cdot \text{RH}$
  - *Exponential equation*: $D_m = c \cdot e^{(d \cdot \text{RH})}$

where a, b, c and d are fitting parameters.

- Thermal conductivity, λ (W/m K): In case of the moisture transport, the value of the thermal conductivity of the LWHB is moisture-dependent, as it was proven in other previous research works [28,29]. Specifically, for a density of 1329 kg/m^3, we have used the following equation to reproduce this nonlinear thermal behavior [11]:

$$\lambda(\text{RH}) = 2.329757 \cdot \lambda_{50\%} \cdot F_m(\text{RH}) \cdot \frac{1 + 1.001662 \cdot e^{-(\text{RH}/0.124688)}}{1 - 1.08309 \times 10^{-5} \cdot e^{-(\text{RH}/0.124688)}} \tag{6}$$

where

Please cite this article in press as: J.J. del Coz Díaz, et al., Hygrothermal study of lightweight concrete hollow bricks: A new proposed experimental–numerical method, Energy Buildings (2013), http://dx.doi.org/10.1016/j.enbuild.2013.11.060

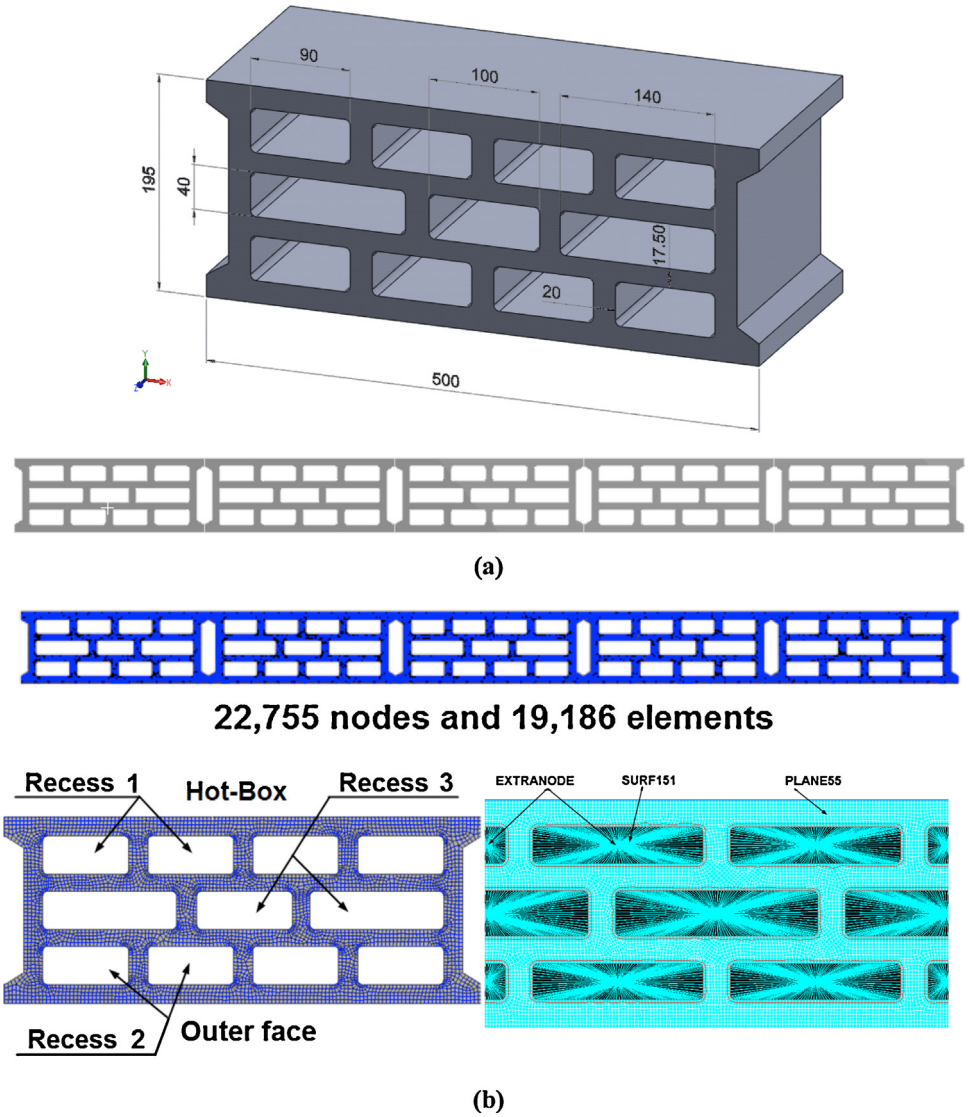

Fig. 6. Geometrical and FEM models of the LWHB: (a) single brick and assembled five bricks; and (b) FEM mesh, a brick mesh detail and finite element types used.

- RH is the relative humidity content in the material (%) and $\lambda_{50\%}$ is the thermal conductivity for a 50% relative humidity content. Its value is 0.2541 W/m K.
- F_m is a conversion factor for the moisture content experimentally obtained, derived from the standard rule UNE-EN ISO 10456 [30]:

$$F_m(\mathrm{RH}) = 6.0105 \times 10^{-9}\mathrm{RH}^3 + 3.2273 \times 10^{-6}\mathrm{RH}^2 + 6.1979 \times 10^{-4}\mathrm{RH} + 0.96216 \times e^{4.3323\times10^{-5}\mathrm{RH}} \quad (7)$$

3.3. Geometrical and FEM models

In order to obtain the moisture and temperature distributions of a wall made up of light concrete bricks, two-dimensional geometrical models have been built using five LWHBs and keeping constant its external length (2.500 m) and width (0.195 m) (see Fig. 6(a)). Note that the real dimensions of the wall (1 m × 1 m) are different than in the numerical model. However, this FEM methodology, based on our previous research works [31,32], is reliable and accurate enough by using the numerical results in the central brick.

The geometrical models described above was meshed using a meshing parameter of 4 mm (see Fig. 6(b)) with the following finite elements [33–35]:

- *Plane 55 element*: it is a four node thermal-solid element and one degree of freedom in each node. It is used in the solid part of the brick to simulate the moisture transport as well as thermal conduction.
- *Surf 151 element*: it is a three node thermal surface effect element (2 nodes + 1 extra node to take into account the convection and radiation effects). This element is overlapped on the plane 55 elements and is used to reproduce the thermal and moisture transport in each one of recesses or cavities of the bricks.

3.4. Numerical analyses and boundary conditions

Based on the previous FEM model, the following numerical analyses corresponding to the hygrothermal laboratory tests (see Fig. 2) have been carried out:

A1: Stabilization analysis
A2: Drying analysis
A3: Thermal analysis.

Please cite this article in press as: J.J. del Coz Díaz, et al., Hygrothermal study of lightweight concrete hollow bricks: A new proposed experimental–numerical method, Energy Buildings (2013), http://dx.doi.org/10.1016/j.enbuild.2013.11.060

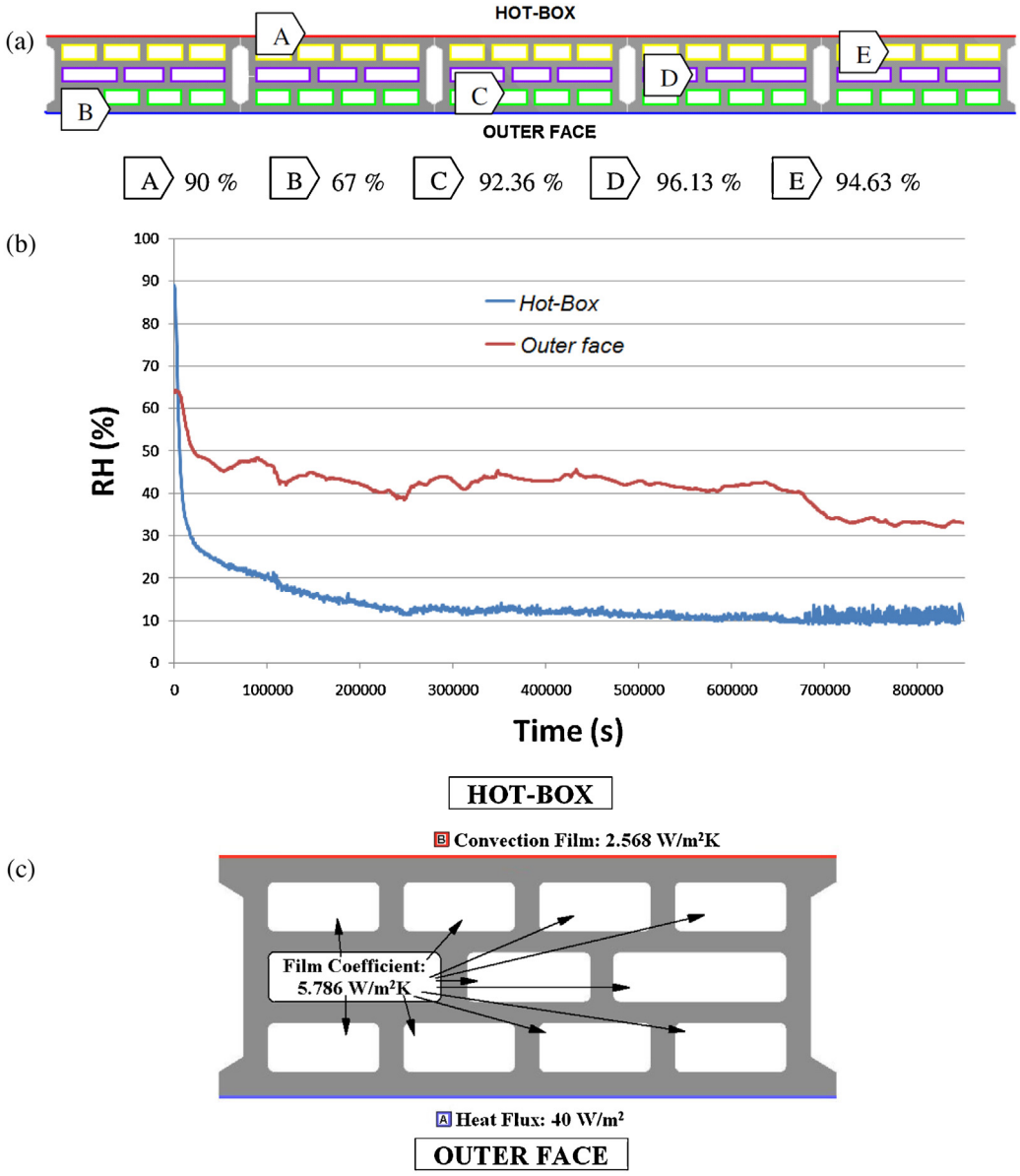

Fig. 7. FEM boundary conditions for: (a) moisture transport analysis A1; (b) moisture transport analysis A2; and (c) thermal analysis A3.

In order to solve the entire hygrothermal boundary value problem (HBVP), two different boundary value problems (BVPs) are tackled:

- Firstly, Eq. (4), corresponding to the moisture transport, with the following boundary conditions:
  - BC1: The initial RH measured in lab on the outer face (outside), inner face (hot-box) and recesses is applied in the FEM model, as it is indicated in Fig. 7(a) for the A1 stage.
  - BC2: The RH evolution over 864,000 s (10 days) measured in lab is specified on the outer face (outside) and inner face (hot-box) (see Fig. 7(b)) for the A2 stage.
  - BC3: The internal boundary condition in the recesses for the A2 stage are implemented through the equivalent moisture film coefficient, h_{coz}, in the following way:

$$q_{coz} = h_{coz} \cdot A \cdot (m_i - m_j) \quad (8)$$

- Finally, Eq. (5), corresponding to the thermal analysis stage A3, is solved from the previous moisture transport results, with the following boundary conditions:
  - BC4: Based on the lab conditions, a heat flux of 40 W/m^2 on the inner face and a film coefficient of 2.568 W/m^2 K on the outer face are imposed (see Fig. 7(c)).
  - BC5: The convective and radiative thermal transports inside recesses are replaced by a convective equivalent empirical thermal flow according to the standard rule EN-ISO-6946:~~1996~~[36], giving place to an equivalent film coefficient of 5.786 W/m^2 K ~~[37]~~.

The nonlinear discrete problem was solved by a dual Intel Xeon E5630 Workstation, with 16 cores, 64 GB of RAM and 4 TB hard disk. The CPU times correspondig to A1–A3 numerical analyses were 35 s, 1600 s and 1300 s, respectively. Additionally, the A1 and A3 analyses were solved using a Newton–Raphson integration scheme while the A2 analysis used the incomplete Cholesky conjugate gradient (ICCG) solver with a tolerance of 10^{-8} (stopping criterion) and an implicit time integration scheme (backward Euler method).

Please cite this article in press as: J.J. del Coz Díaz, et al., Hygrothermal study of lightweight concrete hollow bricks: A new proposed experimental–numerical method, Energy Buildings (2013), http://dx.doi.org/10.1016/j.enbuild.2013.11.060

Table 2
Input variables and its ranges of variation (A1 and A2 analyses).

	Initial value	Minimum value	Maximum value
Recess 1, h_{coz}^{R1}	0.145	0.100	0.170
Recess 2, h_{coz}^{R2}	1.500	1.300	2.800
Recess 3, h_{coz}^{R3}	0.145	0.100	0.170
Specific heat moisture coefficient	4600	4230	5170
Moisture diffusivity law, fitting parameter c	0.380	0.350	0.420
Moisture diffusivity law, fitting parameter d	−0.017	−0.019	−0.015

Table 3
Q3 GDO numerical results (A1 and A2 analyses).

	Candidate points				
	Candidate A	Candidate B	Candidate C	Candidate D	Candidate E
RMSE Recess-1	16.8205	16.7756	16.9454	17.0530	16.6802
RMSE Recess-2	13.1288	13.2486	12.9420	12.8354	13.3306
RMSE Recess-3	8.1138	8.0338	8.2294	8.1319	8.1153
Overall RMSE	**13.1721**	13.1732	13.1738	13.1757	13.1780
Parameter c	**0.3957**	0.4121	0.3631	0.4072	0.3843
Parameter d	**−0.0153**	−0.0167	−0.0156	−0.0164	−0.0182
Specific Heat (J kg^{-1} C^{-1})	**4973.19**	4849.40	4601.83	4694.67	4508.99
h_{coz}^{R1}	**0.1023**	0.1112	0.1045	0.1028	0.1017
h_{coz}^{R2}	**1.3226**	1.3280	1.3116	1.4101	1.4320
h_{coz}^{R3}	**0.1314**	0.1063	0.1628	0.1090	0.1672

4. Numerical results and DOE optimization

Using the finite element method (FEM) in combination with the design of experiments (DOE) methodology, it is possible to determine the optimal parameters of the model in order to obtain the best fitting to the experimental results. In this sense, this research work uses an innovative numerical technique named as "goal driven optimization" (GDO) [21]. The GDO framework uses a decision support process (DSP) based on satisfying criteria as applied to the parameter attributes using a weighted aggregate method. In effect, the DSP can be viewed as a postprocessing action on the response surfaces generated from the design of experiments analyses.

On the one hand, the DOE analysis gives place to 46 different FEM models based on a central composite design (CCD) method, that is to say, a total of 46 different FEM models.

On the other hand, the GDO uses a screening approach. The screening approach is a non-iterative direct sampling method by a quasi-random number generator based on the Hammersley algorithm [22]. In this research work, the equivalent empirical terms are approached using the design of experiments (DOE) technique from the experimental tests ~~[23,31,38]~~ with 1000 sample points (from DOE–FEM results) generated by screening method.

4.1. Stabilization and drying results

From the A1 and A2 analyses, the results corresponding to the moisture distribution inside LHWB are obtained (Fig. 8):

In order to get the best agreement between the experimental and numerical moisture distributions inside bricks, a GDO approach based on FEM–DOE analysis has been carried out. In this sense, it was possible to select the best 5 candidate points from the 1000 sample points generated by the screening method. In this research work, the root mean square error (RMSE) ~~[39]~~ was used as a reliable statistical estimator of the goodness-of-fit looking for the minimum difference between the numerical and experimental relative humidity values in each cavity measured in the laboratory (see the experimental results in Fig. 3(a)). Keeping in mind the selection of the best fitting parameters, then we calculate the overall RMSE considering all the recesses located inside the middle brick.

The input variables considered in the DOE analysis are shown in Table 2 for the exponential moisture-diffusivity approach.

Table 4
Numerical and experimental hygrothermal results.

Time (s)	RH (%)	Numerical results			Experimental results		
		U (W/m^2 K)	R (m^2 K/W)	λ_{eq} (W/m K)	U (W/m^2 K)	R (m^2 K/W)	λ_{eq} (W/m K)
5000	58.11	2.046	0.62881	0.31011	2.039	0.630	0.309
10,000	47.98	1.999	0.64026	0.30456	2.011	0.637	0.306
15,000	42.72	1.972	0.64705	0.30137	1.999	0.640	0.305
25,000	38.07	1.945	0.65406	0.29814	1.977	0.646	0.302
50,000	34.64	1.913	0.66283	0.29419	1.949	0.653	0.299
100,000	33.71	1.875	0.67341	0.28957	1.939	0.656	0.297
200,000	28.13	1.832	0.68572	0.28437	1.852	0.680	0.287
300,000	27.87	1.820	0.68937	0.28287	1.847	0.681	0.286
400,000	27.65	1.816	0.69061	0.28236	1.842	0.683	0.286
500,000	27.42	1.814	0.69122	0.28211	1.838	0.684	0.285
600,000	26.24	1.812	0.69174	0.28190	1.811	0.692	0.282
650,000	25.71	1.812	0.69185	0.28185	1.798	0.696	0.280
700,000	23.08	1.810	0.69242	0.28162	1.726	0.719	0.271
800,000	22.03	1.809	0.69287	0.28144	1.693	0.731	0.267
850,000	21.74	1.809	0.69292	0.28142	1.698	0.729	0.267

Please cite this article in press as: J.J. del Coz Díaz, et al., Hygrothermal study of lightweight concrete hollow bricks: A new proposed experimental–numerical method, Energy Buildings (2013), http://dx.doi.org/10.1016/j.enbuild.2013.11.060

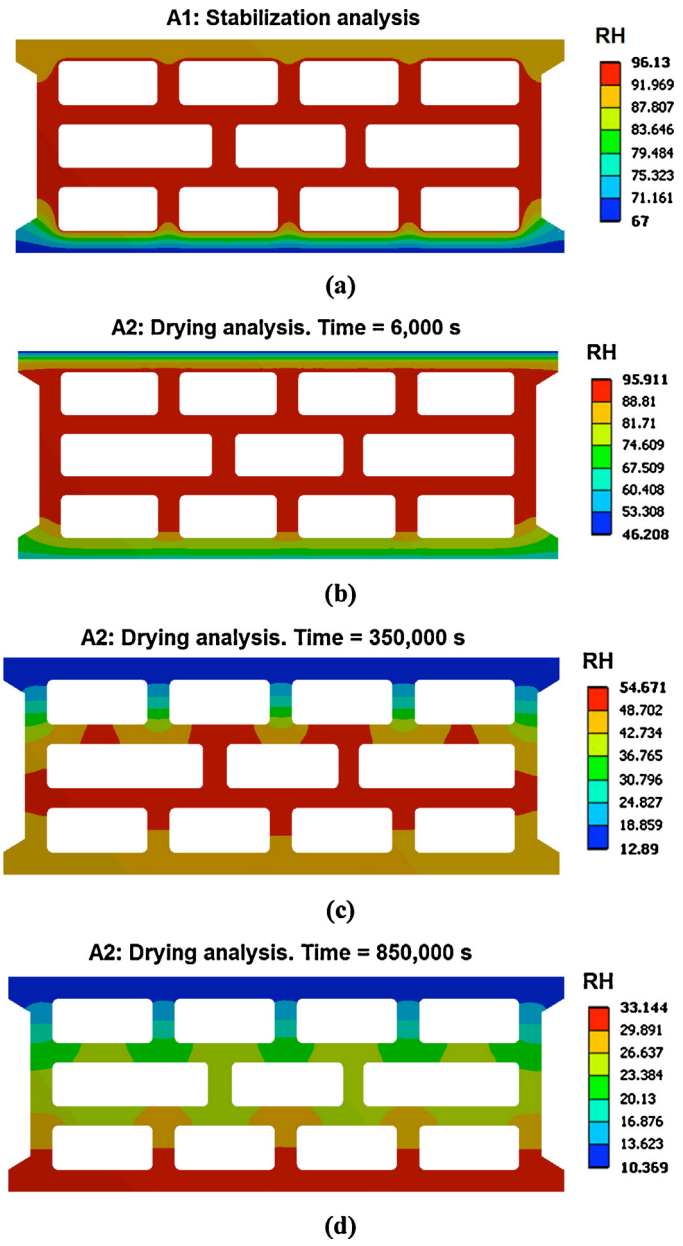

Fig. 8. Numerical moisture distribution results in the middle brick for the A1 and A2 analyses: (a) stabilization stage; (b) drying result for a time equal to 6000 s; (c) drying result for a time equal to 350,000 s; and (d) drying result for a time equal to 850,000 s.

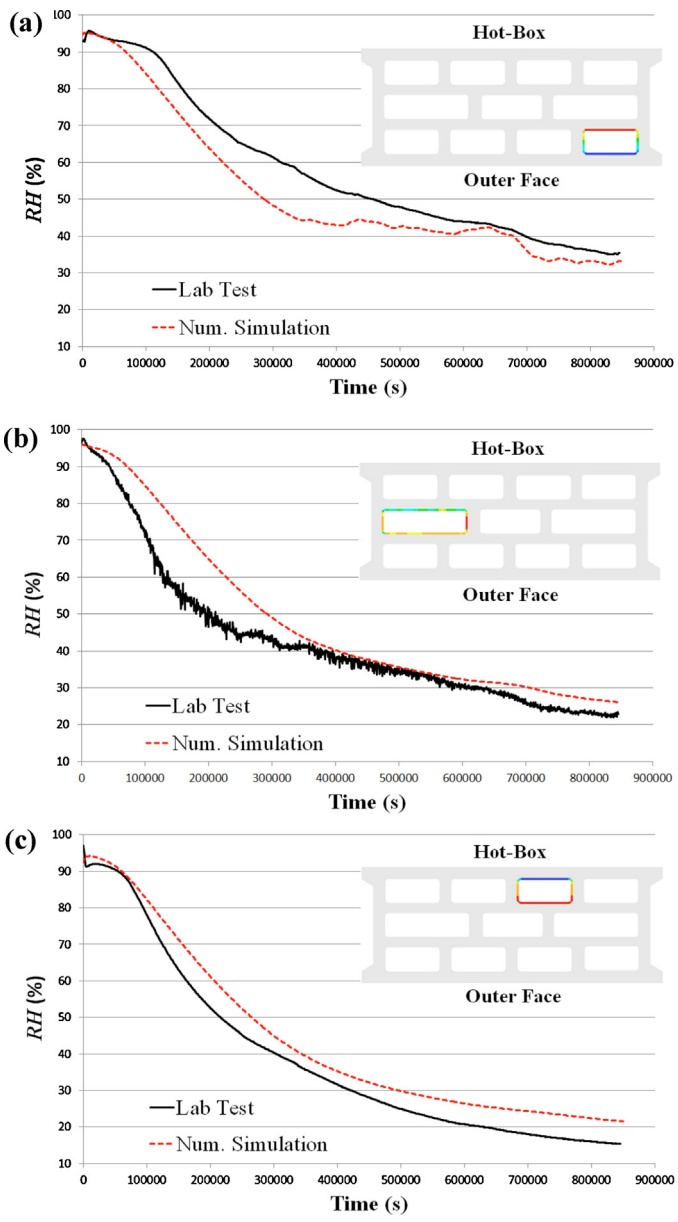

Fig. 9. Numerical and experimental moisture distribution results in the middle brick during the A2 drying analysis for the: (a) recess 1; (b) recess 2; and (c) recess 3.

In this context, Table 3 shows the GDO numerical results. The best candidate point, which corresponds to the minimum value of the overall RMSE estimator, is the candidate A. It is possible to observe that the worst fit corresponds to the recess 1 (a RMSE value equal to 16.8), close to the outer face of the brick, and the best fit to the recess 3 (a RMSE value equal to 8.1), near the hot-box. Additionally, Fig. 9 indicates the numerical and experimental moisture distributions in the drying stage for the inner, outer and middle recesses.

4.2. Hygrothermal results

From the results corresponding to the previous moisture distribution, the material thermal conductivity of each finite element is updated in 15 time periods using advanced programming design language (APDL) [33–35]. Fig. 10 shows the material properties in each finite element for different times: 5000 s, 400,000 s and 800,000 s, respectively (each color corresponds to a different thermal conductivity).

Next, the thermal boundary conditions are applied and the governing equation (Eq. (5)) is solved.

Once the problem has been solved, the temperature distribution in the bricks is obtained for the different time steps (see Fig. 11). Then, the inner and outer faces of the middle brick are selected in order to calculate the following main brick thermal properties [40,41]:

$$U = \frac{Q}{\Delta T} \quad (9)$$

$$R = \frac{1}{U} + R_{se} + R_{si} \quad (10)$$

$$\lambda_{eq} = \frac{e}{R} \quad (11)$$

The numerical and experimental hygrothermal results corresponding to the thermal transmittance, overall thermal resistance

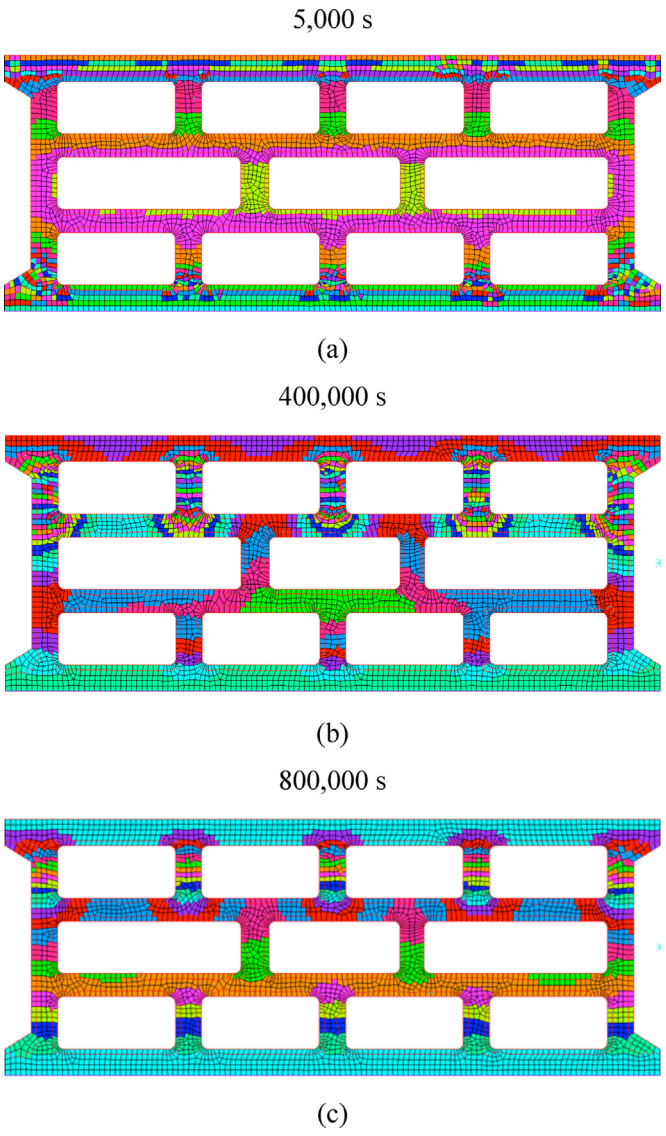

Fig. 10. Material thermal conductivities in each finite element for different times: (a) 5000 s; (b) 400,000 s; and (c) 800,000 s.

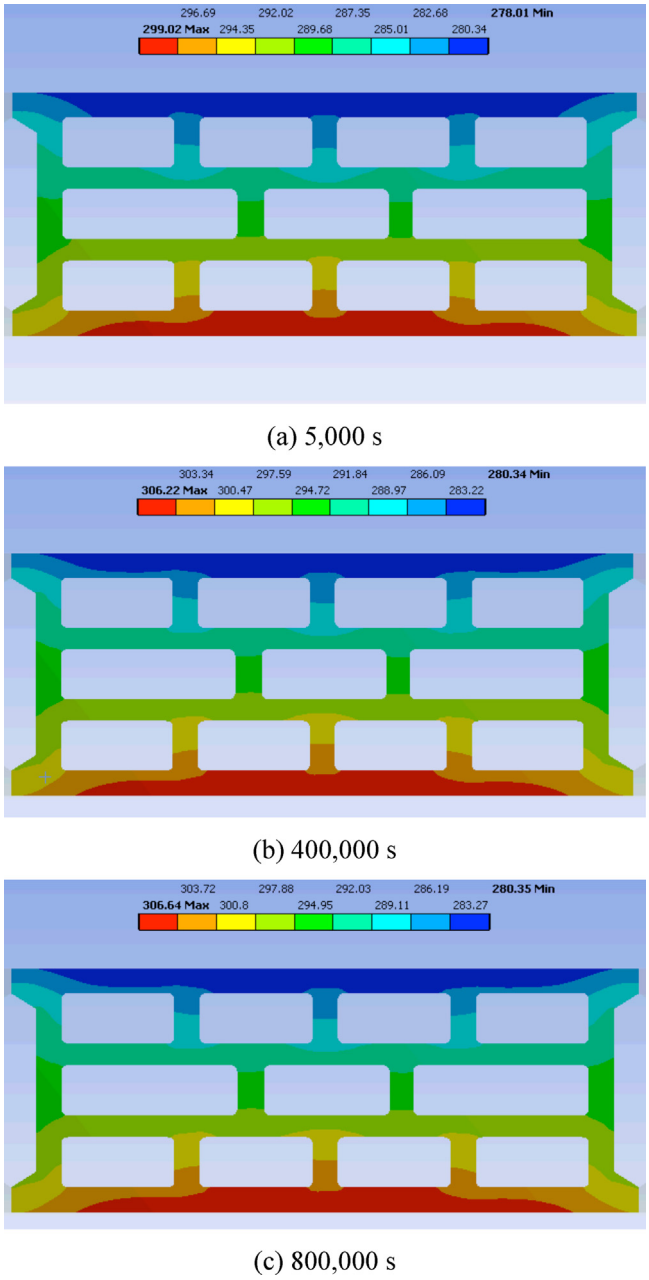

Fig. 11. Numerical temperature distribution results in the middle brick for different lab test times: (a) 5000 s; (b) 400,000 s; and (c) 800,000 s.

and equivalent thermal conductivity for the 15 time periods are shown in Table 4. Furthermore, Fig. 12 indicates the comparison between the experimental and numerical heat transmission coefficients as a function of the relative humidity.

Keeping in mind, the goodness-of-fit, the RMSE statistical estimator is calculated from the numerical and experimental thermal transmittance values shown in Table 4 and Fig. 12. In this way, the RMSE using the FEM model described previously in this paper is 0.0539. Therefore, it is possible to assert that the numerical and experimental results are in a good agreement.

Finally, the prime novelty of this research work is that the overall methodology used for the entire hygrothermal problem allows to propose the following golden rule according to the results of this research work: it is possible to solve the entire hygrothermal behavior of bricks carrying out only the stabilization and drying stages. In consequence, only 480 h of laboratory tests are necessary instead of 1488 h. This gives place to energy and time savings close to 70% with respect to the actual test procedures.

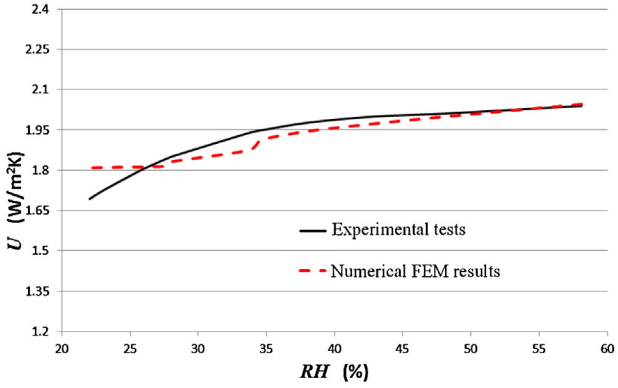

Fig. 12. Experimental and numerical thermal transmittance curves as a function of the relative humidity.

Please cite this article in press as: J.J. del Coz Díaz, et al., Hygrothermal study of lightweight concrete hollow bricks: A new proposed experimental–numerical method, Energy Buildings (2013), http://dx.doi.org/10.1016/j.enbuild.2013.11.060

5. Conclusions

In summary, the following main findings have been reached:

- Firstly, a generic finite element formulation to solve the hygrothermal boundary value problem (HBVP) was developed for the lightweight hollow bricks (LWHBs). The coupled theoretical model by Philip and De Vries for the moisture and heat transport in porous media was simplified using the Fick's law based on the physical analogy between the moisture transport and heat transfer.
- Secondly, seven hypotheses (H1–H7) have been considered in order to build an uncoupled mathematical model to solve the heat and moisture transport through unsaturated LWHBs. The partial differential governing equations are based on driving potentials of temperature and moisture gradients, while radiation-convective boundary conditions inside the inner recesses of bricks were applied.
- Thirdly, a two-dimensional model of a wall made up of five hollow bricks was implemented to obtain the moisture and temperature distributions of the LWHBs. The geometrical model has been discretized using a two-dimensional thermal solid finite element with four nodes and a single degree of freedom at each node (relative humidity and temperature), and a thermal surface effect element with 3 nodes (2 nodes + 1 extra node included). This nonlinear discrete problem was solved using an implicit time integration scheme (backward Euler method) in combination with a Newton–Raphson integration scheme and the incomplete Cholesky conjugate gradient (ICCG) solver.
- Fourthly, an experimental setup was implemented in our lab using a 1 cm^3 hot-box connected to a special climatic chamber. In order to measure the thermal flux, the temperature and relative humidity distributions in a one square meter wall, a total of 32 sensors were used. These experimental tests have allowed to fit and improve the mathematical models using a goal design optimization (GDO) technique based on the FEM analysis and design of experiments (DOE) technique.
- Fifthly, very good agreements were found between the predicted and measured thermal performances of the wall subjected to a different moisture conditions. Therefore, the current model is accurate and able to predict the hygrothermal transfer in porous materials including air domains. Note that the presence of recesses or cavities (air domains inside bricks) implies an additional complexity not solved numerically until now.
- Finally, this hybrid methodology based on the numerical and experimental mixture can be applied to other similar coupled problems in the field of the hygrothermal transport with success. Specifically, this procedure has allowed energy and time savings of approximately 70% with respect to the real test procedures.

The coupled heat and moisture transfer in porous building materials is a very complex phenomenon. There are some subjects requiring additional researches. Future studies will be mainly focused on two directions:

- The additional development of the current model, focused on the hygrothermal behavior at microscopic level, which will help to understand better the moisture and heat transfer phenomena in porous media.
- Extra future experiments and numerical analyses applied to other construction materials are required in order to check the validity of the proposed hybrid method.

Even though the model developed here assumes several hypotheses, it has been proved that in case of the lightweight concrete multi-holed bricks, this hybrid method was a very useful tool to obtain a high accuracy with respect to the real tests [24,25,30,36,41].

Uncited reference

[42].

Acknowledgments

The authors acknowledge the partial funding from the Gijon City Council through the SV-13-GIJON-1.7 project. Furthermore, the financial support provided by the FICYT and the Spanish Ministry of Science and Innovation through the following research projects co-financed with FEDER funds is considered: FC-10-EQUIP10-17, PC-10-33, BIA2008-00058 and BIA2012-31609. Furthermore, we also thank the manufacturer MAXIT Ltd. for the bricks provided and finally, to Swanson Analysis Inc. for the use of ANSYS University Research program.

References

[1] M. Qin, A. Aït-Mokhtar, R. Belarbi, Two-dimensional hygrothermal transfer in porous building materials, Applied Thermal Engineering 30 (16) (2010) 2555–2562.
[2] D. Gawin, J. Kosny, A. Desjarlais, Effect of moisture on thermal performance and energy efficiency of buildings with lightweight concrete walls, in: Proceedings ACEEE Summer Study on Energy Efficiency in Buildings, vol. 3, 2000, pp. 3149–3160.
[3] X. Lu, Modelling of heat and moisture transfer in buildings, I. Model program, Energy and Building 34 (2002) 1033–1043.
[4] E. Yasar, Y. Erdogan, Strength and thermal conductivity in lightweight building materials, Bulletin of Engineering Geology and the Environment 67 (4) (2008) 513–519.
[5] H.Z. Cui, T. Yiu Lo, S. Ali Memon, W. Xu, Effect of lightweight aggregates on the mechanical properties and brittleness of lightweight aggregate concrete, Construction and Building Materials 35 (2012) 149–158.
[6] J.M. Perez-Bella, J. Dominguez-Hernandez, B. Rodriguez-Soria, J.J. Del Coz Diaz, E. Cano-Suñen, Estimation of the exposure of buildings to driving rain in Spain from daily wind and rain data, Building and Environment 57 (2012) 259–270.
[7] J.M. Perez-Bella, J. Dominguez-Hernandez, B. Rodriguez-Soria, J.J. Del Coz Diaz, E. Cano-Suñen, Optimised method for estimating directional driving rain from synoptic observation data, Journal of Wind Engineering and Industrial Aerodynamics 113 (2013) 1–11.
[8] J.C. Zanchet Piaia, M. Cheriaf, J. Cavalcante Rocha, N. Luperont Mustelier, Measurements of water penetration and leakage in masonry wall: experimental results and numerical simulation, Building and Environment 61 (2013) 18–26.
[9] J.J. Del Coz Díaz, A. Lozano Martínez-Luengas, J.M. Adam, A.M. Rodríguez, Non-linear hygrothermal failure analysis of an external clay brick wall by FEM – a case study, Construction and Building Materials 25 (12) (2011) 4454–4464.
[10] B. Blocken, D. Derome, J. Carmeliet, Rainwater runoff from building facades: a review, Building and Environment 60 (2013) 339–361.
[11] J.J. Del Coz Díaz, F.P. Álvarez Rabanal, P.J. García Nieto, J. Domínguez Hernández, B. Rodríguez Soria, J.M. Pérez-Bella, Hygrothermal properties of lightweight concrete: experiments and numerical fitting study, Construction and Building Materials 40 (2013) 543–555.
[12] P. Talukdar, S.O. Olutmayin, O.F. Osanyintola, C.J. Simonson, An experimental data set for benchmarking 1D, transient heat and moisture transfer models of hygroscopic building materials. Part I. Experimental facility and material property data, International Journal of Heat and Mass Transfer 50 (23–24) (2007) 4527–4539.
[13] A. Al-Sibahy, R. Edwards, Thermal behaviour of novel lightweight concrete at ambient and elevated temperatures: experimental, modelling and parametric studies, Construction and Building Materials 31 (2012) 174–187.
[14] J.J. Del Coz Díaz, P.J. García Nieto, A. Martín Rodríguez, A. Lozano Martínez-Luengas, C. Betegón Biempica, Non-linear thermal analysis of light concrete hollow brick walls by the finite element method and experimental validation, Applied Thermal Engineering 26 (8–9) (2006) 777–786.
[15] K. Abahri, R. Belarbi, A. Trabelsi, Contribution to analytical and numerical study of combined heat and moisture transfers in porous building materials, Building and Environment 46 (7) (2011) 1354–1360.
[16] A. Bouchair, Steady state theoretical model of fired clay hollow bricks for enhanced external wall thermal insulation, Building and Environment 43 (10) (2008) 1603–1618.
[17] L.P. Li, Z.G. Wu, Y.L. He, G. Lauriat, W.Q. Tao, Optimization of the configuration of 290 × 140 × 90 hollow clay bricks with 3D numerical simulation by finite volume method, Energy and Buildings 40 (10) (2008) 1790–1798.
[18] A. Luikov, Heat and Mass Transfer in Capillary Porous Bodies, Pergamon Press, Oxford, 1966, pp. 240–250.

Please cite this article in press as: J.J. del Coz Díaz, et al., Hygrothermal study of lightweight concrete hollow bricks: A new proposed experimental–numerical method, Energy Buildings (2013), http://dx.doi.org/10.1016/j.enbuild.2013.11.060

[19] J. Philip, D. De Vries, Moisture movement in porous materials under temperature gradients, Transactions, American Geophysical Union 38 (1957) 222–232.
[20] M. Khoshbakht, M.W. Lin, C.A. Feickert, A finite element model for hygrothermal analysis of masonry walls with FRP reinforcement, Finite Elements in Analysis and Design 45 (2009) 511–518.
[21] W. Chen, M. Sim, Goal-driven optimization, Operations Research 57 (2) (2007) 342–357.
[22] U.M. Diwekar, J.R. Kalagnanam, Efficient sampling technique for optimization under uncertainty, AIChE Journal 43 (2) (1997) 440–447.
[23] J.J. Del Coz Díaz, P.J. García Nieto, F.P. Álvarez Rabanal, A. Lozano Martinez-Luengas, Optimization based on design of experiments (DOE) using finite element model (FEM) analysis applied to retrofitting the church of Baldornon, Spain, International Journal of Architectural Heritage 6 (4) (2011) 436–451.
[24] ASTM C 1363 – 05, Standard test method for the thermal performance of building assemblies by means of a Hot Box apparatus.
[25] UNE-EN ISO 8990:1997, Thermal insulation. Determination of steady-state thermal transmission properties. Calibrated and guarded hot-box (ISO 8990:1994).
[26] S. Ferrari, V. Zanotto, The thermal performance of walls under actual service conditions: evaluating the results of climatic chamber tests, Construction and Building Materials 4 (2013) 309–316.
[27] H. Kus, E. Özkan, Ö. Göcer, E. Edis, Hot box measurements of pumice aggregate concrete hollow block walls, Construction and Building Materials 38 (2013) 837–845.
[28] Y.A. Cengel, Heat and Mass Transfer, McGraw-Hill College, New York, 2007.
[29] M.W. Lin, J.B. Berman, M. Khoshbakht, Modeling of moisture migration in a FRP reinforced masonry structure, Building and Environment 41 (5) (2006) 646–656.
[30] G.H. Dos Santos, N. Mendes, Heat, air and moisture transfer through hollow porous blocks, International Journal of Heat and Mass Transfer 52 (9–10) (2009) 2390–2398.
[31] J.J. Del Coz Díaz, P.J. García Nieto, L.M. Díaz Pérez, J. Domínguez Hernández, P. Riesgo Fernández, Nonlinear thermal analysis of multi-holed lightweight concrete blocks used in external and non-habitable floors by FEM, International Journal of Heat and Mass Transfer 54 (1–3) (2011) 533–548.
[32] J.J. Del Coz Diaz, P.J. Garcia Nieto, J. Dominguez Hernandez, A. Suarez Sanchez, Thermal design optimization of lightweight concrete blocks for internal oneway spanning slabs floors by FEM, Energy and Buildings 41 (12) (2009) 1276–1287.
[33] I. Sandberg, Effects of moisture on the thermal performance of insulating materials, in: Moisture Control in Buildings: The Key Factor in Mold Prevention, H.R. Trechsel and M.T. Bomberg, New York, 2009.
[34] UNE-EN ISO 10456:1999, Building materials and products. Procedures for determining declared and design thermal values (ISO 10456:1999).
[35] S. Moaveni, Finite Element Analysis: Theory and Applications with ANSYS, Prentice Hall, New York, 2003.
[36] E. Madenci, I. Guven, The Finite Element Method and Applications in Engineering Using ANSYS, Springer, Berlin, 2005.
[37] K.L. Lawrence, ANSYS Tutorial 10, Schroff Development Corporation, New York, 2005.
[38] UNE-EN ISO 6946:2012, Building components and building elements. Thermal resistance and thermal transmittance. Calculation method (ISO 6946:2007).
[39] J.J. Del Coz Díaz, P.J. Garcia Nieto, D. Castro-Fresno, P. Menéndez Rodríguez, Steady state numerical simulation of the particle collection efficiency of a new urban sustainable gravity settler using design of experiments by FVM, Applied Mathematics and Computation 217 (2011) 8166–8178.
[40] J.J. Del Coz Díaz, P.J. García Nieto, A. Lozano Martínez-Luengas, J.L. Suárez Sierra, A study of the collapse of a WWII communications antenna using numerical simulations based on design of experiments by FEM, Engineering Structures 32 (2010) 1792–1800.
[41] P. Dunesche, B. Remillard, Statistical Modeling and Analysis for Complex Data Problems, Springer, New York, 2010.
[42] UNE-EN ISO 7345:1996 (ISO 7345:1987), Thermal insulation. Physical quantities.

Please cite this article in press as: J.J. del Coz Díaz, et al., Hygrothermal study of lightweight concrete hollow bricks: A new proposed experimental–numerical method, Energy Buildings (2013), http://dx.doi.org/10.1016/j.enbuild.2013.11.060